Visible light 3D printing with epoxidized vegetable oils

Diego Savio Branciforti[a,b], Simone Lazzaroni[a,b,c], Chiara Milanese[d], Marco Castiglioni[a], Ferdinando Auricchio[e,b], Dario Pasini[f,b] and Daniele Dondi[a,b]

[a] University of Pavia, Department of Chemistry, Inorganic Chemistry Section, Viale Taramelli 12, 27100 Pavia, Italy

[b] Consorzio Interuniversitario Nazionale per la Scienza e Tecnologia dei Materiali (INSTM), Via G. Giusti 9, 50121 Florence, Italy

[c] Laboratory of Applied Nuclear Energy, LENA, University of Pavia, Via Aselli 41, 27100 Pavia, Italy

[d] University of Pavia, C.S.G.I. & Department of Chemistry, Physical Chemistry Section, Pavia H_2 Lab, Viale Taramelli 16, 27100, Pavia, Italy

[e] University of Pavia, Department of Civil Engineering and Architecture, Via Ferrata 3, 27100 Pavia, Italy

[f] University of Pavia, Department of Chemistry, Organic Chemistry Section, Viale Taramelli 12, 27100 Pavia, Italy

Corresponding author:
Daniele Dondi
University of Pavia
Department of Chemistry
Viale Taramelli 12, 27100, Pavia, Italy
Phone: +39 382 987344
Fax: +39 382 528544
Email: **daniele.dondi@unipv.it**

Abstract
Stereolithography is a 3D printing technique in which a liquid monomer is photopolymerized to produce a solid object. The most widely used materials usually belong to the family of acrylate monomers, and photopolymerization occurs through a radical pathway. Photoinitiators can absorb UV or (less often) visible light, producing radicals for direct decomposition or hydrogen abstraction. Due to the toxicity of acrylates, vegetable oil-derived monomers were used in this study. In fact, vegetable oils contain unsaturations, and thus, they can be exploited as monomers. In particular, linseed oil, tung oil or edible oils (soybean, sunflower or corn) could be good candidates as raw materials. Unfortunately, the photoinduced radical polymerization of these oils

either does not occur or is too slow for 3D printing applications. For this reason, the oils were modified as epoxides. Epoxides are monomers that are more reactive than natural oils, and they can be polymerized via a cationic mechanism. The aim of this work was to exploit visible light generated by a common digital projector (like those used in classrooms) as a light source. Since the tested photoacid generators working under visible light are ineffective for the polymerization of epoxidized oils, a multi-component photo-initiating mixture was used.

Keywords
Visible light stereolithography; vegetable oil epoxides; photoinduced cationic polymerization; ring opening polymerization; green resins.

1. Introduction

Additive manufacturing, usually known as 3D-printing, is a technique introduced a few decades ago to manufacture objects, mainly for prototyping. The technique has been widely used in the last two decades, through the adoption of open-hardware and software approaches, leading to the introduction of the so-called RepRap machines, in which all the plastic parts of the printer can be created by the printer itself. In fact, RepRap machines could be built for less than the price of a laptop PC. Several techniques are used for the creation of an object: the widely used fused deposition modelling (FDM), selective laser sintering (SLS), light-induced (including laser) photopolymerization (also called stereolithography, STL) and inkjet printing, and combinations of the techniques are also used. Currently, 3D-printing has become useful for scientists, starting from the building of custom labware [1-2] as well as dedicated chemical reactors [3]. In addition, electronic circuits [4] or microwave devices [5] can be realized with this technique. Moreover, the introduction of bottom-up manufacturing permits us to tailor technological applications, such as lithium-ion batteries [6]; in particular, 3D-printing is of special interest when it is used to build materials that cannot be produced under conventional fabrication techniques, such as metamaterials [7] or ultra-stiff materials [8]. Other applications are related to medical applications, such as tissue engineering or bone reconstruction and the use of living cells as materials (bioprinting) [9-14], or the fabrication of autonomous soft robots [15]. To compile an exhaustive list of all the possibilities opened by 3D-printing is not possible, and these are only some recent examples taken from the literature. It is noteworthy that chemical research can provide new materials to be used for novel applications and new technologies are being exploited every day. For example, the introduction of a new technique leading to speed enhancement, together with other improvements, received attention in scientific literature [16] as well as from the media. Surprisingly, only a few studies have deepened our understanding of the possible release of toxic substances such as volatile organic compounds (VOCs) or fine particles during printing [17-19], and these studies are related mainly to two (ABS and PLA) of the possible plastic filaments. Moreover, 3D printed parts obtained both from FDM and STL can also show toxicity towards zebrafish embryos [20]. The toxicity of STL printed objects depends on the curing process after printing. In fact, printed objects are cured with UV light after printing and this treatment can reduce

their toxicity. However, the treatment does not completely eliminate the toxicity of these parts. This could be related to the presence of residual acrylate (and methacrylate) monomers, since they are well known toxic compounds [21] for inhalation, swallowing and skin contact. Acrylates are known to cause cytotoxicity, cardiovascular failure, gastrointestinal problems, respiration issues, and developmental malformations [22-23]. However, most of the widely used resins available on the market for 3D printing are acrylates photoinitiated with type I or type II photoinitiators [24] (e.g., resins for dental applications).

For this reason, we considered using modified vegetable oils as monomers. Vegetable oils by themselves, excluding siccative oils, possess very low reactivity towards photopolymerization. Vegetable oils represent a renewable resource that can be used as reliable monomers, but many of the applications are based on their acrylate derivatives ready for radical polymerization [25-26]. To increase the reactivity of oils, while keeping an eye on their toxicity, their epoxides were considered instead in this paper. In fact, epoxidized vegetable oils are greener alternatives that are suitable for producing epoxy resins and thermosetting materials [27,28]. Epoxide polymerization can be undergone via cationic ring-opening polymerization. Thanks to recent advances in the field [29], it is possible to trigger polymerization with a standard digital projector.

2. Materials and methods

Reagents are commercially available from Sigma Aldrich (Italy). Vegetable oils were bought at the local store and used without further purification. Visible light photoacid generators (PAGs) Irgacure PAG 103 and Irgacure PAG 121 were kindly supplied by BASF.

^{1}H-NMR spectra were recorded with a Bruker AV-300 300 MHz spectrometer in $CDCl_3$. The IR spectra were recorded with a Perkin Elmer 1600 FT-IR Spectrophotometer equipped with Specac Golden Gate attenuated total reflectance (ATR). Differential scanning calorimetry (DSC) analyses were performed by heating approximately 20 mg of the samples in an Al pan at 5°C/min from - 90°C to 300°C under nitrogen flux in a Q2000 apparatus provided by TA Instruments. To obtain Photo-DSC analyses, the DSC was modified using 3D printed components (see below). Thermogravimetric analyses (TGA) were performed with a Mettler Toledo-TGA 1 Star^{e} System. The sample was placed in an alumina crucible. The temperature programme was a heating ramp from 25°C to 800°C at a rate of 10°C/min. Nitrogen was used as a carrier gas (4 L/min) and background (a run performed in the same conditions with an empty crucible) was subtracted from the measurement.

2.1. Photo-DSC apparatus

The photo-DSC apparatus is composed of a plano convex lens (focal length 100 mm, diameter 12.7 mm), one LED (nominal wavelength 405 nm; viewing angle 120°; electrical power 4830 mW), and 3D printed supports. The distance LED-lens is 100 mm, while the lens focus is positioned at the bottom of the aluminium crucible. For each measurement, 30-40 mg of the

samples was used. Photo-DSC analyses were performed in isothermal conditions at 30°C under argon flux. The plano convex lens and the LED are commercially available from ThorLabs.

2.2. Experimental stereolithographic apparatus

The experimental stereolithographic apparatus is made up of a data projector HDMI IBM M400 with the following features: resolution 1024 x 768 pixels, lamp (electrical) power 120 W, light intensity 1100 lumens; a plano convex lens (focal length 150 mm, diameter 70 mm); a front-surface mirror and a stepper-driven vertical motion system (Figure 6). The dimension of the projection area was 47 x 65 mm. The apparatus is controlled by software written by us in Python, running on a Raspberry Pi. It allows us to project layers of sectioned objects and to control the movement of the platform. Section images were calculated using Slic3r software.

2.3. Epoxidation of Vegetable oils

The procedure was adapted from reference [30]. In a 500-mL three-necked flask equipped with condenser, thermometer and dropping funnel, 100 g of vegetable oil and 13.97 g of formic acid were heated and stirred at 45°C - 55°C. When the system reached this range of temperature, 0.5 mL of sulfuric acid 98%w was added as a catalyst, and then. 116.98 g hydrogen peroxide solution 35%w in H_2O was gradually dropped into the mixture during the first phase of reaction (for Tung oil, 160 g of H_2O_2 solution were used instead). The temperature was kept between 45°C - 55°C. The molar ratio of natural oil: formic acid: H_2O_2 is 1:2.64:8.9. When all the H_2O_2 was added, the reaction was allowed to continue for 4-5 hours at 55°C.

Then, the system was cooled down to 25°C. During this period, the mixture separated into two parts. Subsequently, by using a separating funnel, the mixture was washed with distilled water and sodium bicarbonate solution (5 g/200 mL) repeatedly until its pH was equal to 7.0.

Then, ethyl acetate was added to the organic phase. Brine solution was added in order to remove excess water in the organic phase. The cloudy solution was then dried with anhydrous magnesium sulfate at ambient temperature. After 2 hours, the clear mixture was filtered and the solvent was removed by vacuum evaporation.

2.4. Photopolymerizable epoxide composition photocatalysed with a radical photoinitiator

The formulation of the solution was adapted from reference [31]. In 5.64 g of epoxidized vegetable oil, 0.066 g of phenylbis(2,4,6-trimethylbenzoyl) phosphine oxide (BAPO), 0.12 g of diphenyliodonium hexafluorophosphate (IOD1), or bis(4-methylphenyl)iodonium hexafluorophosphate (IOD2), or bis(4-tert-butylphenyl)iodonium hexafluorophosphate (IOD3) and 0.25 mL tris-(trimethylsilyl) silane (TTMSS) were dissolved. A small quantity of Sudan I (S1), i.e., 125 μL of S1 stock solution (10 mg/mL), was added. The solution was submitted to ultrasounds for 0.5 h. The quantity of S1 can be varied between 0.005 and 0.4 mg/mL to adjust the thickness of the layers, with an inverse relationship existing between the quantity of S1 and the thickness of the layers.

2.5. Photopolymerizable epoxide composition photocatalysed with curcumin
The formulation of the solution was adapted from reference [31]. In 5.82 g of epoxidized vegetable oil, 0.066 g of curcumin, 0.12 g of diphenyliodonium hexafluorophosphate (IOD1), or bis(4-methylphenyl)iodonium hexafluorophosphate (IOD2), or bis(4-tert-butylphenyl)iodonium hexafluorophosphate (IOD3) were dissolved. In this case, no dye was added. The solution was submitted to ultrasounds for 0.5 h and heated at 40°C [32].

2.6. EPR photolysis
EPR spectra were recorded on a Bruker EMX X-band continuous wave spectrometer equipped with an EPR cavity Bruker ER4102ST. Working conditions were amplitude modulation 5 G, microwave power 10 mW, field sweep 200 G and acquisition time 10.5 s for each scan. Irradiation was performed with a focussed lamp (Osram HBO 100 W Super Pressure Mercury Lamp) with glass lens (the light spot on the cavity is approximately 5 cm in diameter).

3. Results and discussion

3.1. Preliminary experiments
The preliminary experiments allowed us to define the behaviour of the natural oils when they were exposed to the DLP digital projector light. Untreated natural oils, as expected, do not change after an exposure time of 30 minutes. The addition of 2% photoinitiator (BAPO) caused skinning and bleaching only on the Tung oil. In another control experiment, natural oils were mixed with 2% PAG 103 or PAG 121 visible light photoacid generators. As in the previous case, no polymerization occurred after irradiation. Only Tung oil showed the formation of a thin film and a change of colour, going from yellow to red/brown in the irradiated area.
Preliminary experiments showed that the oils need to be chemically modified for the applications of 3D printing. The chosen chemical modification was epoxidation to improve the characteristics of the natural oils.

3.2. Epoxidation
Epoxidation reaction conditions were optimized. A minimum temperature of 45°C was found to start the reaction, since temperatures higher than 55-60°C lead to a reduced formation of epoxide, likely due to its thermal decomposition and partial polymerization. In Figure 1, the temperature in the course of the reaction is shown for the exploratory reactor (250 mL) and the production (1000 mL) reactor. As seen (Figure 1), the increase in volume negatively affects the thermal controllability of the reaction. This should be taken into account in the scaling up of the process.
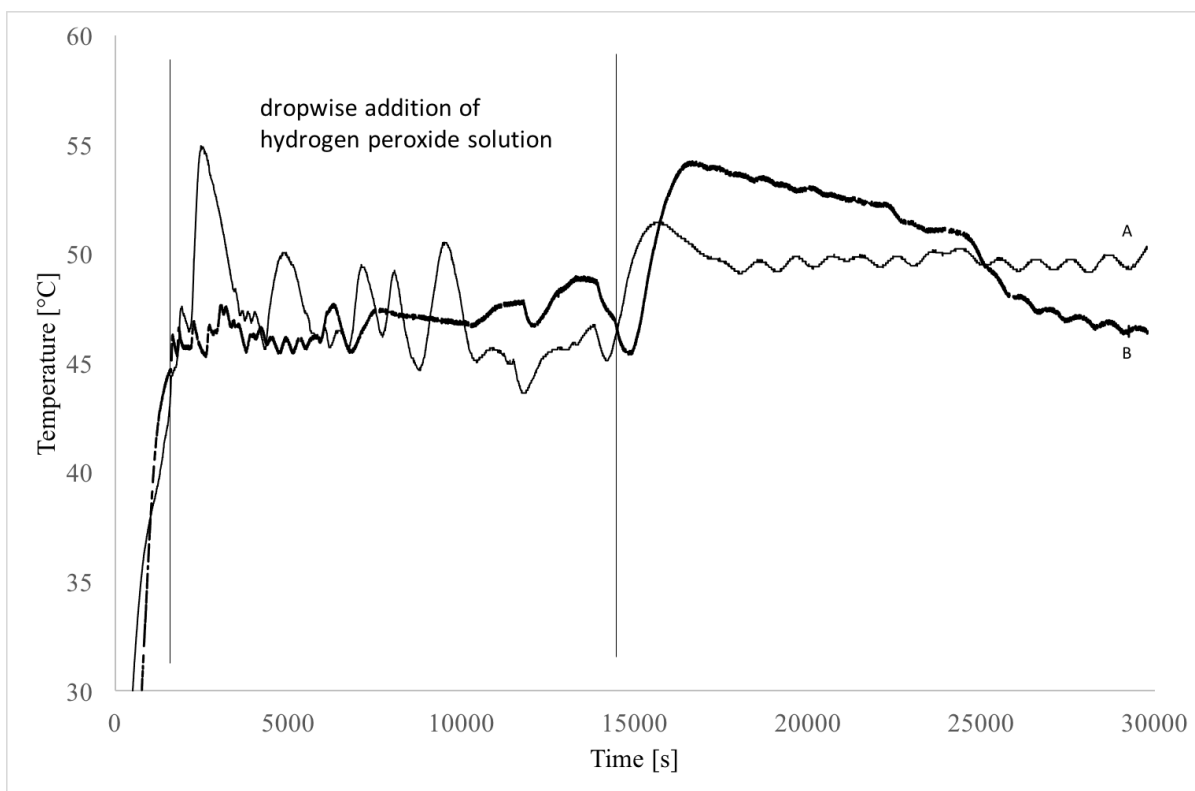
Figure 1. Temperature-time graph for a reaction with a 250-mL (B) and a 1000-mL (A) vessel.

Table 1. Measured internal epoxidation degree of oils and yields of epoxidation.

Starting material	Internal Epoxidation Degree [%]	Epoxidation yield [%][a]
SOYBEAN OIL	90% ± 5%	31%
CORN OIL	89% ± 5%	24%
SUNFLOWER OIL	89% ± 5%	34%
LINSEED OIL	86% ± 5%	25%
TUNG OIL*	33% ± 11%	31%

[a] calculated on the amount of dried epoxide at the end of the process

The internal epoxidation degree (IED) of the natural resins was calculated by considering the ratio between the ^{1}H-NMR integrals of epoxy functional groups (EFG), between 2.9 - 3.1 ppm, and the double bonds (DB) between 5.3 - 5.4 ppm. The IED (Table 1) was calculated using the following equation:

$$IED = \frac{Epoxy\ Functional\ Groups}{(Epoxy\ Functional\ Groups + Double\ Bound)} \cdot 100$$

The epoxidation reactions of Tung oil revealed many problems during the entire process, such as the formations of lumps or the difficulty to separate the epoxidized oil from water.
The ^{1}H-NMR spectra are reported as Supplementary Material.

3.3. Photoinduced cationic polymerization
3.3.1. Method 1
Preliminary tests with PAGs and epoxides gave no detectable amount of polymer, except for skinning. For this reason, the method adopted for polymerization was based on the mechanism of free radical promoted cationic polymerization (FRPCP) [33]. The reaction mechanism (Figure 2) is initiated by an acylphosphinoxide visible-light photoinitiator (BAPO) having a high quantum yield in radical production. The acyl radical generated undergoes hydrogen abstraction on the silane (H-Donor in Figure. 2), giving a silyl radical. Subsequently, the iodonium salt (IOD1 or IOD2 or IOD3) has sufficient oxidation potential to oxidize the silyl radical, giving the silyl cation that is the reactive specie the ability to initiate cationic ring-opening polymerization. The iodonium radical produced after the oxidation underwent a fast decomposition, giving an aryl iodide and aryl radical that ultimately led to benzene formation if IOD1 was used. For this reason, in order to avoid the release of benzene from the polymerized matrix, IOD2 and IOD3 were used instead. It is noteworthy that, in this reaction mechanism, the silane has the dual role of radical intermediate and oxygen scavenger. Nevertheless, TTMSS can be substituted with an equal molar amount of N-vinylcarbazole. In this case, the polymer formed has an increased mechanical stiffness.
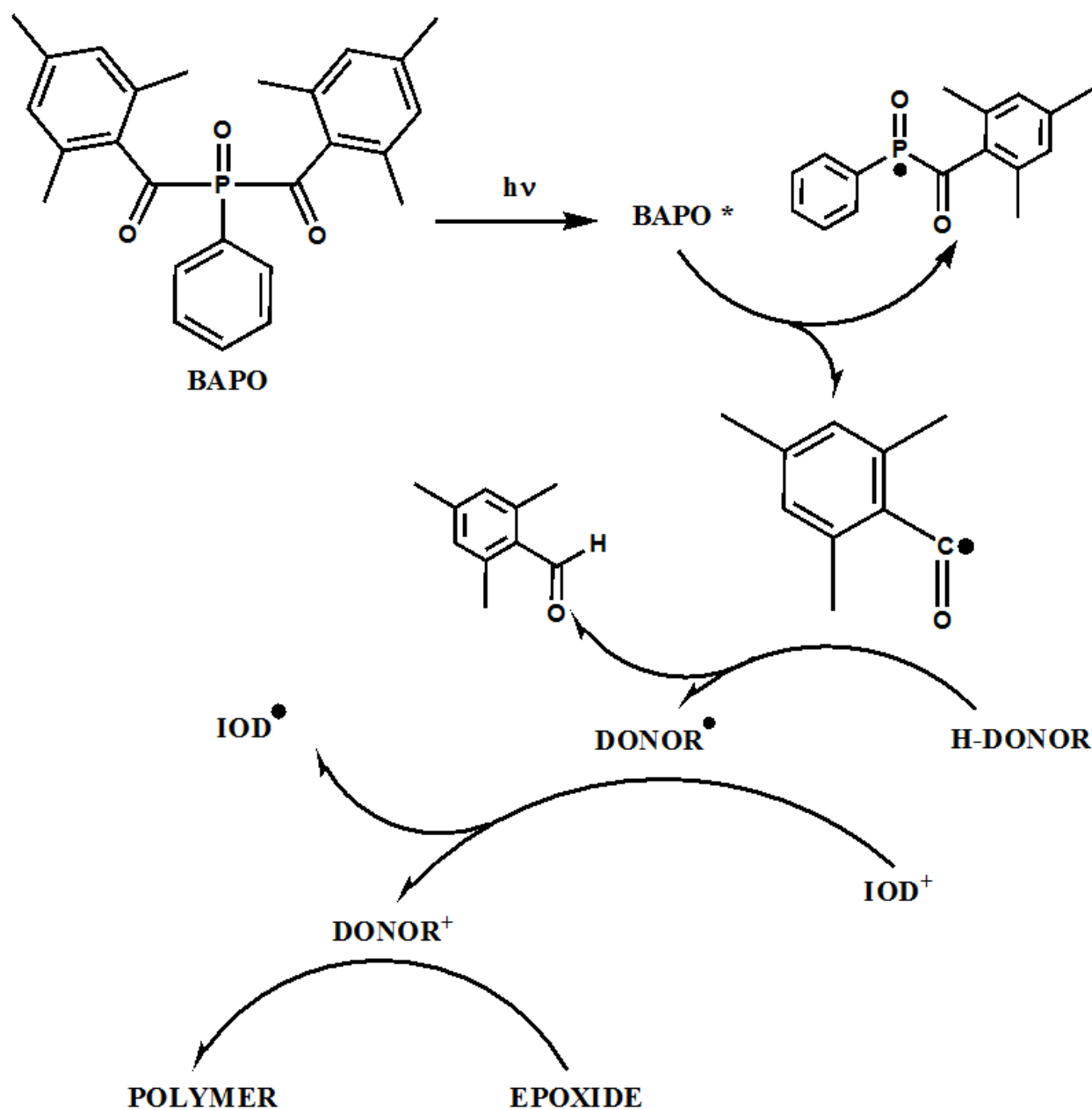
**Figure 2.** Reaction mechanism for the polymerization of epoxides

3.3.2. Method 2

The BAPO/H-donor system can be simplified by using a visible light photosensitizer able to form cations. For this reason, curcumin, a natural occurring dye extracted from the spice turmeric, can be used efficiently [34]. However, curcumin alone is not able to start the polymerization of the epoxides. Nevertheless, the photoreaction of curcumin produces radicals that can be easily oxidized by iodonium salts. For this reason, the complexity of the mixture is reduced and the silane is no longer necessary. Moreover, due to the high absorptivity of curcumin in the visible range, no dye is necessary for efficient printing.

3.4. EPR measurement

The irradiation of a BAPO/silane/iodonium/epoxide mixture in the EPR cavity gave the immediate peak of a silane radical. The radical could survive in the mixture for several minutes after the irradiation was stopped. If the irradiation was prolonged for some minutes, secondary radical species appeared in the centre of the EPR spectrum (carbon-centred radicals), but only when IOD2 was present (Figure 3).
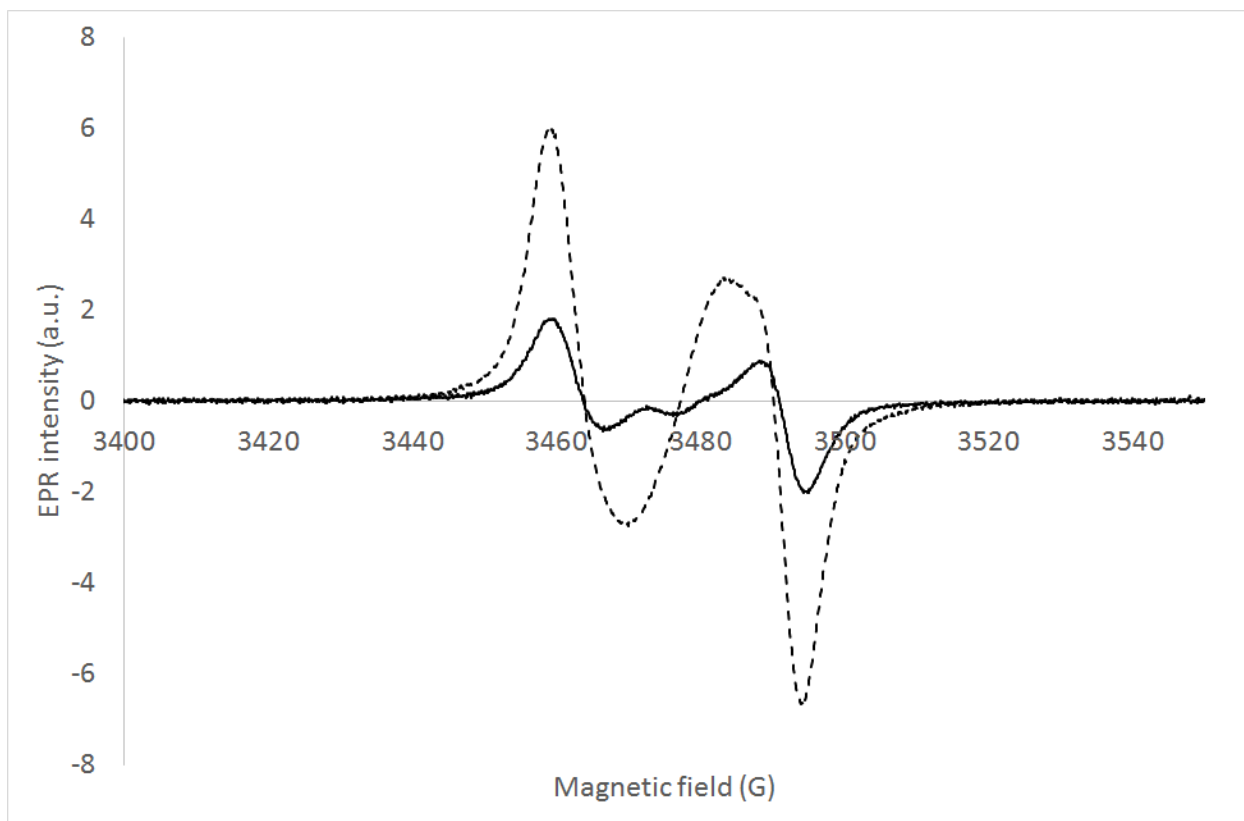
Figure 3. EPR spectrum recorded during irradiation (see text). Dotted line: after 1 s of irradiation; continuous line: after 1 min irradiation.

This dynamic could be related to the formation of benzyl radicals, but due to the poorly resolved spectrum, it was not possible to make a clear attribution.

As seen in Figure 4, the silyl radicals rapidly increased under irradiation, reaching a photostationary equilibrium. At the same time, carbon radicals accumulated in the matrix. When irradiation was stopped, the silyl radicals showed an exponential decay, while the concentration of carbon radicals was stable. It is possible that carbon radicals are localized and blocked in the polymerized part of the mixture, while silyl radicals are reacting with IOD2, producing (cationic) EPR-silent species.
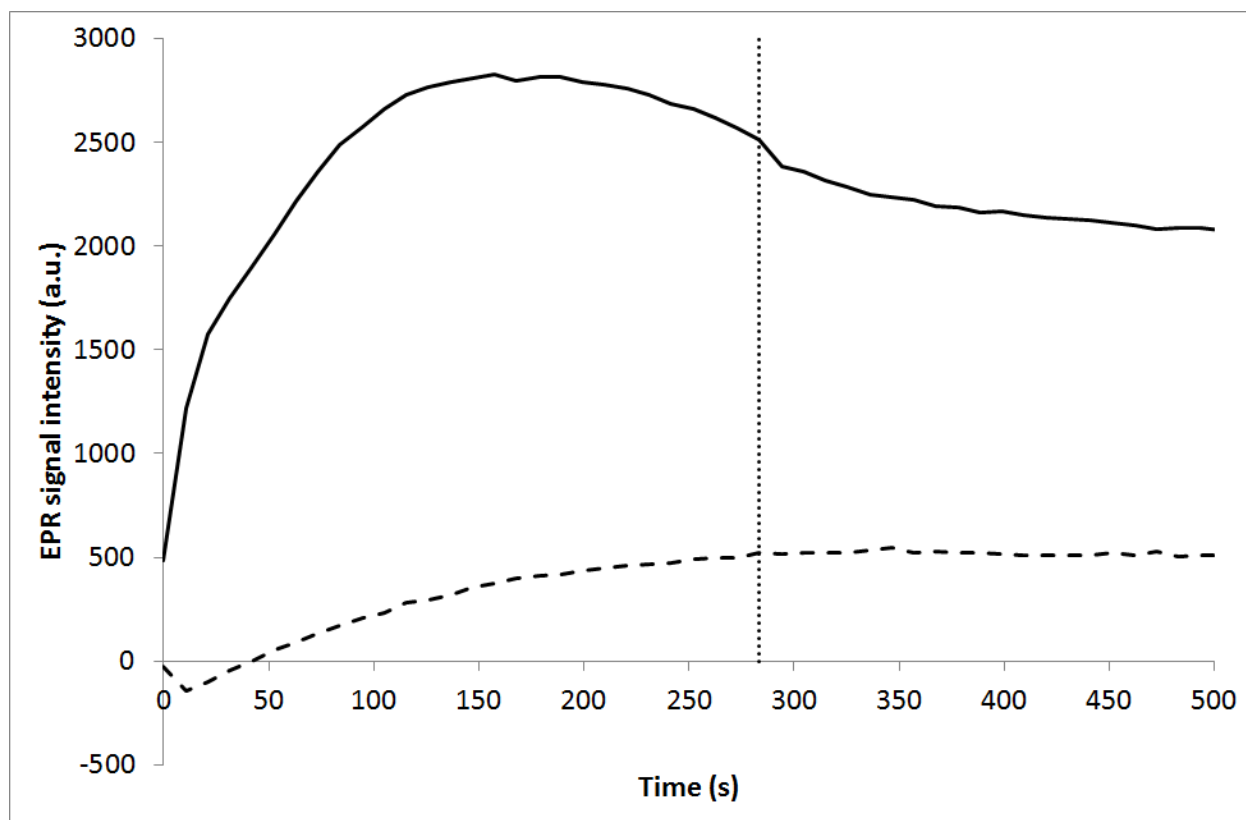
Figure 4. EPR signal intensity of silyl radicals (continuous line) and carbon radicals (dotted line) during irradiation. The vertical line represents the end of irradiation.

When curcumin was used instead of the BAPO/H-donor system, only the radicals derived from curcumin decomposition were visible by EPR, giving a broad singlet (Figure 5). The observed radicals disappeared immediately when the light is turned off.
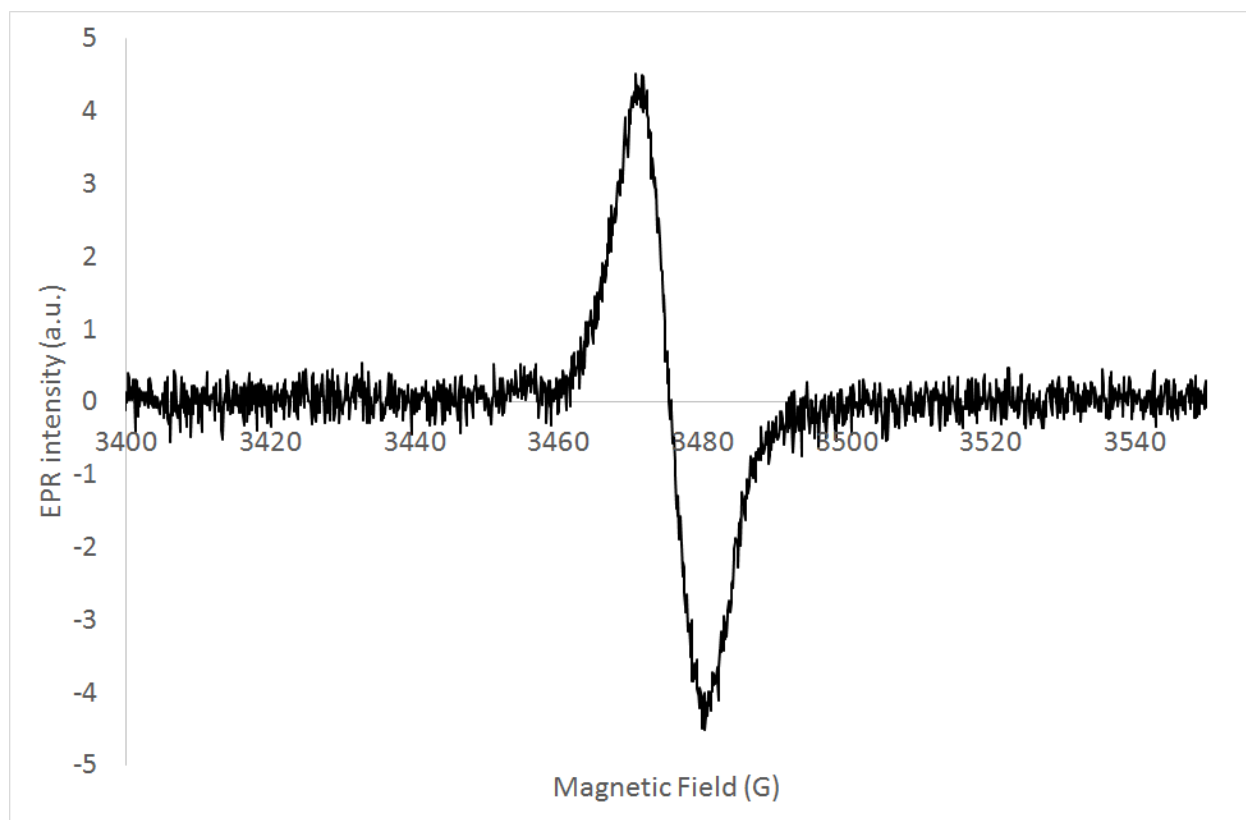
Figure 5. EPR signal obtained during irradiation of the mixture containing curcumin.

3.5. Photo-DSC measurement

Photo-DSC analysis of formulations with BAPO and curcumin were done in isothermal conditions at 30°C under an inert argon atmosphere. The heating due to the focalized light of the LED on the aluminium crucible (0.6 mW) was subtracted from all data. When the LED was turned on, the analysis showed how the samples that contained the BAPO released more energy (2.47-10.43 J/g) than the samples with the curcumin (0.146-0.616 J/g). The same was true for the speed of reaction; indeed, BAPO samples were faster (1200-2400 s) than the curcumin (3600 - 7200 s). All graphics are included in the support material (Figures S6-S10).

3.6. Printing process

A visible light absorber is necessary in order to prevent light from also promoting polymerization in the deeper layers. The amount of the dye influences decisively the time of polymerization. For this reason, different tests were done using three types of natural resins that were obtained by changing the concentration of S1 and timing the polymerization process. In this way, the minimum required quantity of S1 to obtain a perfect level of polymerization was determined. During the three tests, S1 was dosed by adding a stock solution (10 mg/ml) to the natural resin (Table 2).

Table 2. Effect of S1 concentration on time of polymerization.

	Test A S1 concentration 0.117 mg/ml	Test B S1 concentration 0.124 mg/ml	Test C S1 concentration 0.146 mg/ml
Polymerization time [s]	**90 s**	**150 s**	**280 s**

The exposure tests showed that the optimal quantity of S1 to get a good degree of polymerization is 0.117 mg/ml, for an exposure time of 90 s and layer thickness of 0.1 mm.
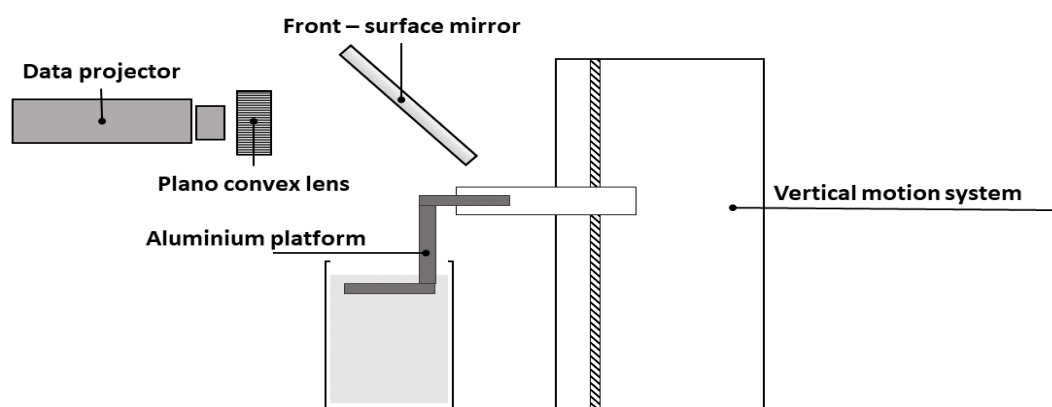
**Figure 6**. Scheme of the apparatus used for 3D printing

Printing tests were done using the system built and optimized by us. The apparatus used is similar to the setup presented by Muskin [35], which is made up of a data projector, a converging lens, a front-surface mirror and a vertical motion system. To improve the control of the printing, a Raspberry Pi was chosen, which allowed us to make the process completely automatic (Figure 6). The clamps and ring stands were used to place the lens and mirror appropriately to ensure an optimal quality of the projected images.

The whole printing process is based on the following steps:

- Exposure. The section image of the model was projected on the surface of the resin for the necessary time to have a complete polymerized layer (Figure 7, a).
- Immersion. After a first sinking of the support for the specified layer height (Figure 7, b), the support was lowered (Figure 7, c) and raised (Figure 7, d) for a few millimetres (3-5 mm). This feature was introduced to resolve the problems related to viscosity of the resins. In fact, the high viscosity and surface tension of the resin made it difficult to form a new layer of liquid on the top of the printed object.

- Settling time. When a new layer of resin was ready, a pause between two consecutive exposures was provided.

The first layer height was manually fixed and a different and long exposure time was used to improve the adhesion to aluminium support of the printed object.
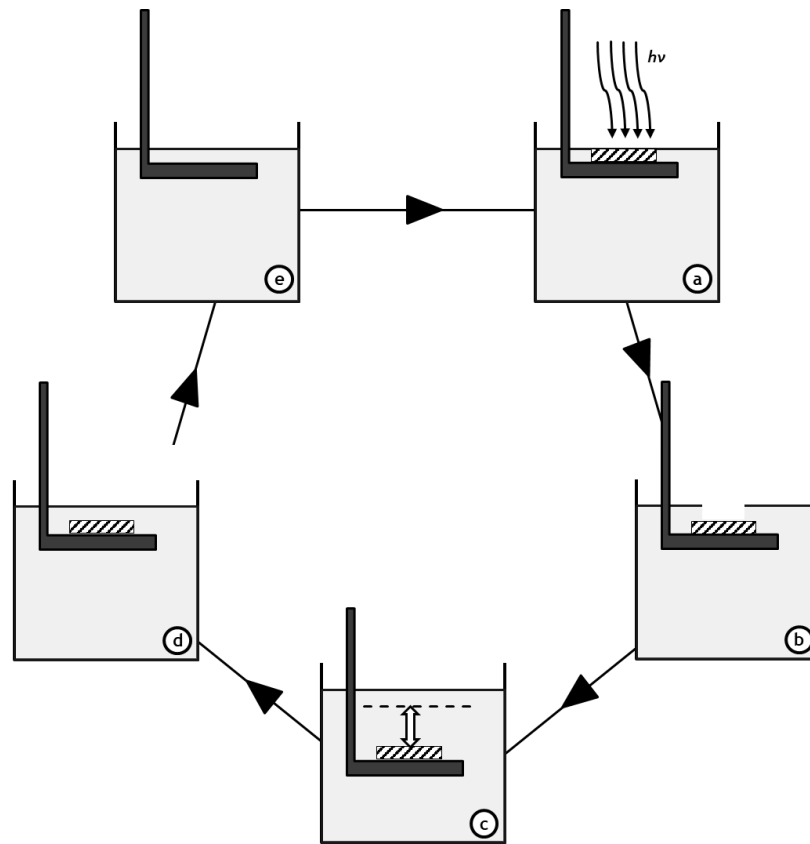
Figure 7. Phases for the printing process: exposure (a), lowering of support (b), sinking (c), emersion (d), settling time (e).

The printed objects showed a good resolution even if the high viscosity of the medium tended to deform the first layers (Figure 9, left), which are subjected to increased stress due to the immersion-emersion system.

Figure 8. Objects printed with linseed oil based resin. Left: neat linseed epoxide (112 layers, 0.2 mm each, 90 s exposure time for each layer), right: linseed epoxide with 20% tri(ethylene glycol) divinyl ether (102 layers, 0.2 mm each, 60 s exposure time for each layer).

To reduce the viscosity of the resin, tri(ethylene glycol) divinyl ether can be added as a cationic reactive diluent. A concentration of 20% by weight was found to be optimal to improve the printability of the material (Figure 9, right).

3.7. Characterization of printed material

The IR spectrum of the polymerized material showed the disappearance of the epoxide ring bands at 821 cm^{-1} and 902 cm^{-1} (Figure 10), in agreement with literature data [36].
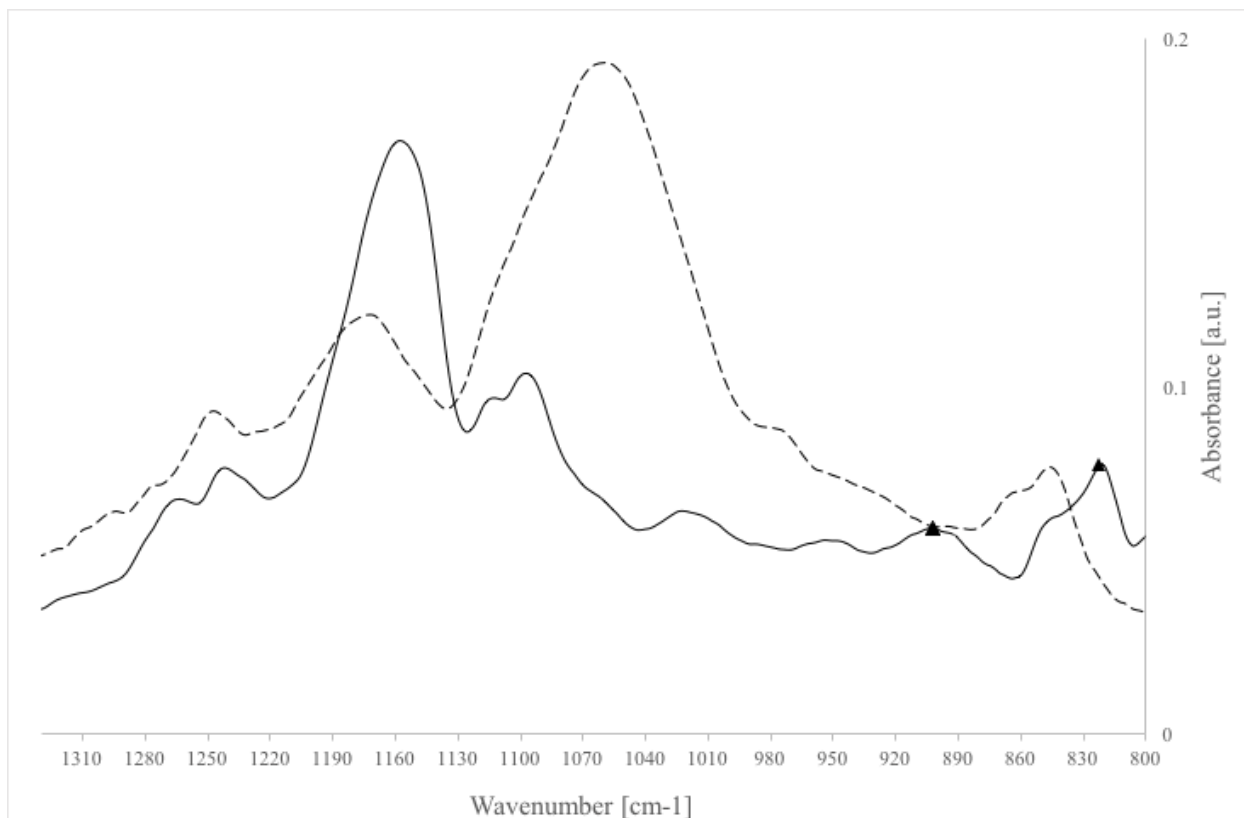
Figure 9. FT-IR spectrum of linseed, epoxidized (dashed line), and polymerized linseed (solid line).

The thermogravimetric analysis, performed under inert gas, showed an initial loss of volatiles (7%) approximately 180°C, probably due to residual initiators. Noticeably, the polymer possessed a high thermal stability and thermal decomposition occurs only at temperatures higher than 350°C (Figure 11).
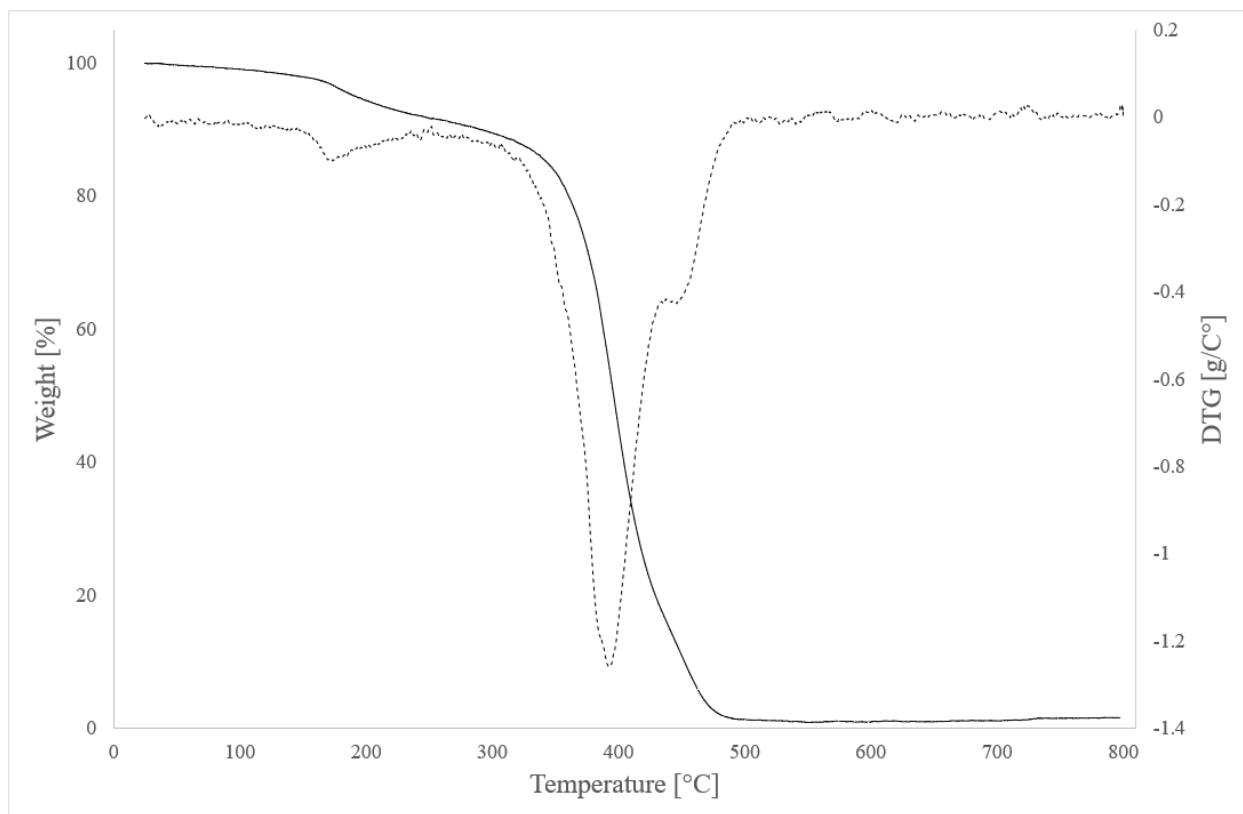
Figure 10. Thermogravimetric analysis (TGA, solid line) and first derivative of the mass signal (DTG, dashed line) of epoxy resin based on linseed oil
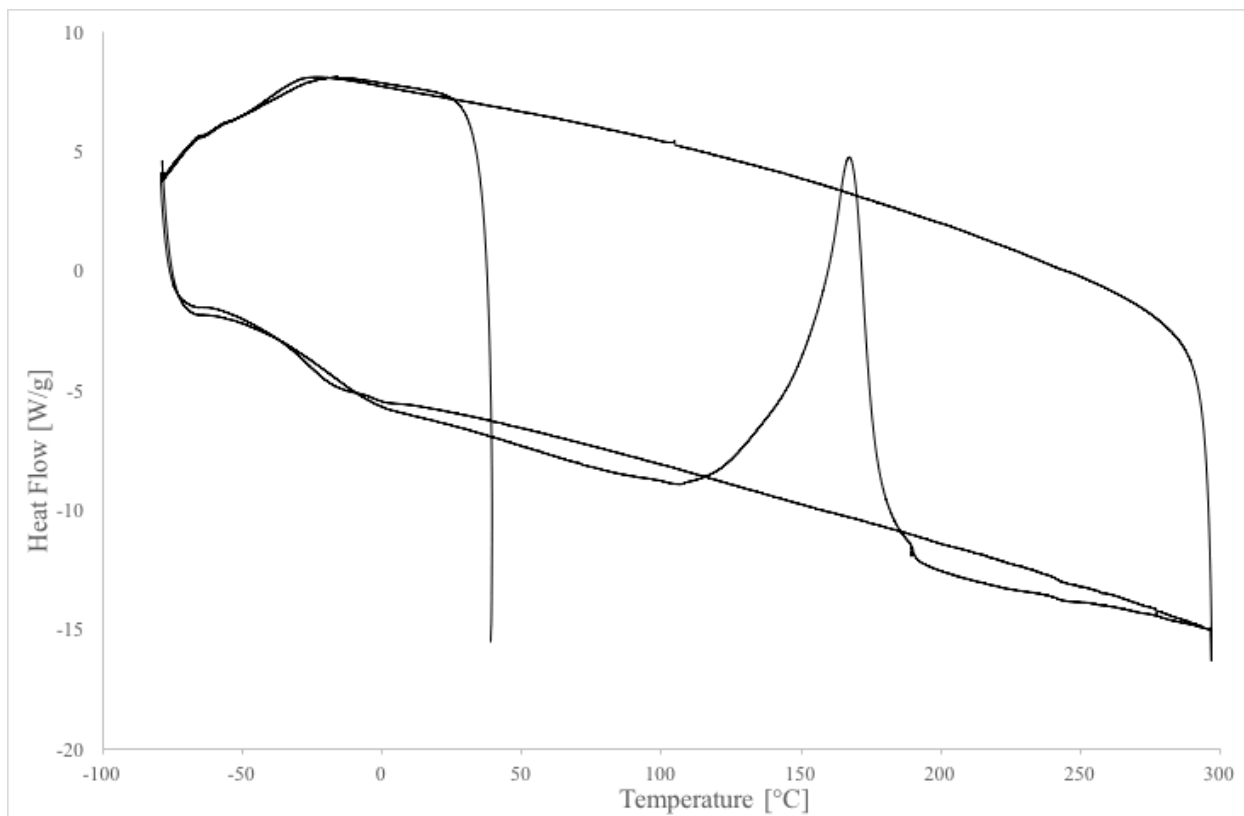
Figure 11. DSC of photopolymerized linseed oil epoxide.

Differential scanning calorimetry (Figure 12) showed that the printed material possessed an exothermic peak approximately 150°C. The peak disappeared during the second heating. This indicated that the polymerization process needs to be completed after the printing (curing). Both thermal curing (70°C for 6 h) and curing by light (the objects were exposed to sunlight for a few days) were investigated. The best results in terms of mechanical resistance were obtained for objects cured slowly under sunlight. From the calorimetric curve, it was also possible to see that the cured polymer possessed a reversible glass transition at approximately -26°C.

4. Conclusion

Vegetable oils without chemical modifications, mixed with the radical or cationic photoinitiators tested, did not undergo polymerization to the extent needed for 3D printing applications. The epoxidation of the oils, together with the FRPCP reaction mechanism, was instead suitable to prepare them for stereolithography. Moreover, a simplified formulation with curcumin and iodonium salts was also effective, even if the exposure time increased. In particular, the best results, in terms of quality of the object printed and durability, were obtained with epoxidized linseed oil as the monomer. Unexpectedly, in our conditions, epoxidized soybean oil was reactive only when TTMSS was replaced by N-vinylcarbazole. To the best of our knowledge, the results presented in this work are the first to exploit vegetable oils' derivatives without acrylates in 3D printing. The biggest issue found was due to the high viscosity of the epoxides that rendered

difficult the formation of a liquid layer over the printed material and ultimately led to shear stress during the printing process. This can be fixed, for example, by admixing different cationic reactive diluents having lower molecular weights.

References

[1] J. M. Pearce, Building research equipment with free, open-source hardware. Science, 2012, 337, 1303–1304.

[2] R. D. Johnson, Custom labware: chemical creativity with 3D printing. Nature Chemistry, 2012, 4, 338-339.

[3] M. D. Symes, P. J. Kitson, J. Yan, C. J. Richmond, G. J. T. Cooper, R. W. Bowman, T. Vilbrandt, L. Cronin, Integrated 3D-printed reactionware for chemical synthesis and analysis. Nature Chemistry, 2012, 4, 349-354.

[4] J. A. Lewis, B. Y. Ahn, Device fabrication: Three-dimensional printed electronics. Nature, 2015, 518, 42-43.

[5] G. McKerricher, M. Vaseem, A. Shamim, Fully inkjet-printed microwave passive electronics. Microsystems & Nanoengineering, Nature, 2017, 3, 16075.

[6] K. Sun, T. S. Wei, B. Y. Ahn, J. Y. Seo, S. J. Dillon, J. A. Lewis, 3D printing of interdigitated Li-ion microbattery architectures, Adv Mater, 2013, 25 (33), 4539-4543.

[7] S. Lee, B. Kang, H. Keum, N. Ahmed, J. A. Rogers, P. M. Ferreira, S. Kim, B. Min, Heterogeneously assembled metamaterials and metadevices via 3D modular transfer printing, Scientific Reports, 2016, 6, 27621.

[8] X. Zheng, H. Lee, T. H. Weisgraber, M. Shusteff, J. DeOtte, E. B. Duoss, J. D. Kuntz, M. M. Biener, Q. Ge, J. A. Jackson, S. O. Kucheyev, N. X. Fang, C. M. Spadaccini, Ultralight, ultrastiff mechanical metamaterials, Science, 2014, 344, 6190, 1373-1377.

[9] S. V. Murphy, A. Atala, 3D bioprinting of tissues and organs, Nature Biotechnology, 2014, 32, 773-785.

[10] B. Derby, Printing and prototyping of tissues and scaffolds, Science, 2012, 338, 6109, 921-926.

[11] N. Cubo, M. Garcia, J. F. del Cañizo, D. Velasco, J. L. Jorcano, 3D bioprinting of functional human skin: production and in vivo analysis, Biofabrication, 2016, 9 (1), 1758-5090.

[12] J. Radhakrishnan, A. Subramanian, U. M. Krishnan, S. Sethuraman, Injectable and 3D bioprinted polysaccharide hydrogels: from cartilage to osteochondral tissue engineering, Biomacromolecules, 2017, 18, 1, 1-26.

[13] C. Mandrycky, Z. Wang, K. Kim, DH. Kim, 3D bioprinting for engineering complex tissues, Biotechnology Advances, 2016, 34(4), 422-434.

[14] G. Gao, X. Cui, Three-dimensional bioprinting in tissue engineering and regenerative medicine, Biotechnology Letters, 2016, 38(2), 203-211.

[15] M. Wehner, R. L. Truby, D. J. Fitzgerald, B. Mosadegh, G. M. Whitesides, J. A. Lewis, R. J. Wood, An integrated design and fabrication strategy for entirely soft autonomous robots, Nature, 2016, 536, 451-455.

[16] J. R. Tumbleston, D. Shirvanyants, N. Ermoshkin, R. Janusziewicz, A. R. Johnson, D. Kelly, K. Chen, R. Pinschmidt, J. P. Rolland, A. Ermoshkin, E. T. Samulski, J. M. DeSimone, Continuous liquid interface production of 3D objects, Science, 2015, 347, 6228, 1349-1352.

[17] Kim, Y., Yoon, C., Ham, S., Park, J., Kim, S., Kwon, O., Tsai, P.J., Emissions of nanoparticles and gaseous material from 3D printer operation. Environ. Sci. Technol. 2015, 49, 12044−12053.

[18] P. Azimi, D. Zhao, C. Pouzet, N. E. Crain, B. Stephens, Emissions of ultrafine particles and volatile organic compounds from commercially available desktop three-dimensional printers with multiple filaments, Environ. Sci. Technol. 2016, 50, 1260−1268.

[19] B. Stephens, P. Azimi, Z. El Orch,T. Ramos, Ultrafine particle emissions from desktop 3D printers. Atmos. Environ. 2013, 79, 334−339.

[20] S. M. Oskui, G. Diamante, C. Liao, W. Shi, J. Gan, D. Schlenk, W. H. Grover, Assessing and reducing the toxicity of 3D-printed parts, Environ. Sci. Technol. Lett. 2016, 3, 1−6.

[21] W. H. Lawrence, G. E. Bass, W. P. Purcell, J. Autian, Use of mathematical models in the study of structure-toxicity relationships of dental compounds: I. Esters of acrylic and methacrylic acids, Journal of Dental Research, 1972, 51, 2, 526-535.

[22] Yoshii, E. Cytotoxic effects of acrylates and methacrylates: relationships of monomer structures and cytotoxicity. J. Biomed. Mater. Res. 1997, 37, 517−524.

[23] Autian, J. Structure-toxicity relationships of acrylic monomers. Environ. Health Perspect. 1975, 11, 141-152.

[24] T. K. Vaidyanathan, J. Vaidyanathan, P. P. Lizymol, S. Ariya, K. K. Venketeswaran, Study of visible light activated polymerization in BisGMA-TEGDMA monomers with Type 1 and Type 2 photoinitiators using Raman spectroscopy, Dental Materials, 2017, 33, 1, 1-11.

[25] G. Lligadas, J. C. Ronda, M. Galià, V. Cádiz, Renewable polymeric materials from vegetable oils: a perspective, Materials Today, 2013, 9, 337-343.

[26] L. Fertier, H. Koleilat, M. Stemmelen, O. Giani, C. Joly-Duhamel, V. Lapinte, J. J. Robin, The use of renewable feedstock in UV-curable materials – A new age for polymers and green chemistry, Progress in Polymer Science, 2013, 38, 932-962.

[27] R. Wang, T. P. Schuman, Vegetable oil-derived epoxy monomers and polymer blends: a comparative study with review, Express Polymer Letters, 2013, 7, 3, 272-292.

[28] S. G. Tan, W. S. Chow, Biobased epoxidized vegetable oils and its greener epoxy blends: a review, Polymer-Plastics Technology and Engineering, 49, 2010, 1581-1590.

[29] J. Lalevee, H. Mokbel, J.P. Fouassier, Recent developments of versatile photoinitiating systems for cationic ring opening polymerization operating at any wavelengths and under low light intensity sources, Molecules, 2015, 20, 4, 7201-7221.

[30] P. Saithai, J. Lecomte, E. Dubreucq, V. Tanrattanakul, Effects of different epoxidation methods of soybean oil on the characteristics of acrylated epoxidized soybean oil-co-poly(methyl methacrylate) copolymer, Express Polymer Letters, 2013, 7(2), 910-924.

[31] M. A. Tehfe, J. Lalevée, D. Gigmes, J. P. Fouassier, Green Chemistry: Sunlight-induced cationic polymerization of renewable epoxy monomers under air, Macromolecules, 2010, 3, 1364-1370.

[32] K. Ahmed, Y. Li, D. J. McClements, H. Xiao, Nanoemulsion- and emulsion-based delivery systems for curcumin: Encapsulation and release properties, Food Chemistry, Issue 2, 15 May 2012, 799-807.

[33] M. A. Tehfe, F. Louradour, J. Lalevée, J. P. Fouassier, Photopolymerization reactions: on the way to a green and sustainable chemistry, Applied Science, 2013, 3(2), 490-514.

[34] J. V. Crivello, U. Bulut, Curcumin: A naturally occurring long-wavelength photosensitizer for diaryliodonium salts, Journal of Polymer Science: Part A: Polymer Chemistry, 5217-5231 (2005).

[35] J. Muskin, M. Ragusa, T. Gelsthorpe, Three-dimensional printing using a photoinitiated polymer, Journal of Chemical Education, 2010, 87, 5, 512-514.

[36] Z. Liu, S. Z. Erhan, Ring-opening polymerization of epoxidized soybean oil, Journal of the American Oil Chemists' Society, 2010, 87, 437-444.